Nigral injection of a proteasomal inhibitor, lactacystin, induces widespread glial cell activation and shows various phenotypes of Parkinson's disease in young and adult mouse

Savolainen, Mari H.

2017-07

Savolainen , M H , Albert , K , Airavaara , M & Myohänen , T T 2017 , ' Nigral injection of a proteasomal inhibitor, lactacystin, induces widespread glial cell activation and shows various phenotypes of Parkinson's disease in young and adult mouse ' , Experimental Brain Research , vol. 235 , no. 7 , pp. 2189-2202 . https://doi.org/10.1007/s00221-017-4962-z

http://hdl.handle.net/10138/307681
https://doi.org/10.1007/s00221-017-4962-z

unspecified
acceptedVersion

Nigral injection of a proteasomal inhibitor, lactacystin, induces widespread glial cell activation and shows various phenotypes of Parkinson's disease in young and adult mouse

Mari H. Savolainen[1], Katrina Albert[2], Mikko Airavaara[2], Timo T. Myöhänen[1*]

[1]Division of Pharmacology and Pharmacotherapy, University of Helsinki, Finland
[2]Institute of Biotechnology, University of Helsinki, Finland

* Corresponding author

E-mail: timo.myohanen@helsinki.fi

Division of Pharmacology and Pharmacotherapy, Viikinkaari 5E, P.O.Box 56, 00014
University of Helsinki, Finland. Tel +358-50-4480769. Orcid ID: 0000-0002-9277-6687

Abstract

Proteinaceous inclusions, called Lewy bodies, are used as a pathological hallmark for Parkinson's disease (PD). Lewy bodies contain insoluble α-synuclein (aSyn) and many other ubiquitinated proteins, suggesting a role for protein degradation system failure in the PD pathogenesis. Indeed, proteasomal dysfunction has been linked to PD but commonly used *in vivo* toxin models, such as 6-OHDA or MPTP, do not have a significant effect on the proteasomal system or protein aggregation. Therefore, we wanted to study the characteristics of a proteasomal inhibitor, lactacystin, as a PD model on young and adult mice.

To study this, we performed stereotactic microinjection of lactacystin above the substantia nigra pars compacta in young (2 month old) and adult (12-14 month old) C57Bl/6 mice. Motor behavior was measured by locomotor activity and cylinder tests, and the markers of neuroinflammation, aSyn and dopaminergic system were assessed by immunohistochemistry and HPLC.

We found that lactacystin induced a Parkinson's disease-like motor phenotype 5-7 days after injection in young and adult mice, and this was associated with wide-spread neuroinflammation based on glial cell markers, aSyn accumulation in substantia nigra, striatal dopamine decrease and loss of dopaminergic cell bodies in the substantia nigra and terminals in the striatum. When comparing young and adult mice, adult mice were more sensitive for dopaminergic degeneration after lactacystin injection that further supports the use of adult mice instead of young when modelling neurodegeneration. Our data showed that lactacystin is useful in modeling various aspects of Parkinson's disease, and taken together, our findings emphasize the role of a protein degradation deficit in Parkinson's disease pathology, and support the use of proteasomal inhibitors as Parkinson's disease models.

Keywords: ubiquitin-proteasome system; proteasome-inhibition; neuroinflammation; neurodegeneration; preclinical models; alpha-synuclein.

Introduction

Parkinson's disease (PD) is the second most common neurodegenerative disease, with an incidence of 1-2% of people over 65 years old. In PD, dopaminergic neurons in the substantia nigra pars compacta (SNc) degenerate, leading to typical clinical findings such as tremor, rigidity and bradykinesia due to lack of dopamine in the striatum. Common neuropathological findings of PD are insoluble inclusions, Lewy bodies, mainly consisting of an α-synuclein (aSyn) protein (Spillantini et al. 1998). Although appearance of Lewy bodies is considered a hallmark for PD, it appears that fibrillary forms of aSyn that are formed during the aggregation process are the toxic species and may be associated with neuronal loss in the SNc (Winner et al. 2011). Current drug therapies are mostly based on dopamine replacement that only relieves the symptoms of PD but are not curative and cannot stop or delay the progress of the disease. Therefore, it is important to develop novel drug therapies and drug candidates, and for this, tools for preclinical studies are needed.

The challenge of generating a mouse model of PD is to find a model that would recapitulate all pathophysiological aspects of the disease: gradual dopaminergic neurodegeneration in the nigrostriatal tract, aSyn-containing protein aggregate formation, motor behavioral deficits and neuroinflammation. Neurotoxin models, 6-OHDA and MPTP, are conventionally used as PD models that show the gradual dopaminergic neurodegeneration and behavioral deficits but 6-OHDA fails to produce substantial protein accumulation in the brain and MPTP administration induces non-fibrillar aggregate formation only after extended administration (Meredith et al. 2002; Fornai et al. 2005; Jin et al. 2005). After revealing that non-soluble aSyn is one of the main components of Lewy bodies (Spillantini et al. 1998) it has been of huge interest to study its role in PD, where it indisputably has a role in the pathogenesis. Since toxin models do not easily produce aSyn-rich protein inclusions, several models that are based on either transgenic or viral vector-mediated overexpression of aSyn have been published (Kahle et al. 2001; Matsuoka et al. 2001; Tofaris et al. 2006; St Martin et al. 2007; Ulusoy et al. 2010; Decressac et al. 2012). Within the models, there is a wide variation of the degree of neuronal degeneration and protein accumulation, and motor behavioral phenotype of these mice is often weak or not present. Very recently, it was shown that when human aSyn is expressed in a mouse carrying normal mouse aSyn, aSyn aggregation is limited compared to overexpressing human aSyn without mouse aSyn homologue (Fares et al. 2016). This finding suggests that synuclein homologs reduce aggregation of each other and offers an explanation on why less toxicity is seen in many transgenic models regardless of high expression.

Although aSyn and its neurotoxic species, oligomers (Winner et al. 2011), have raised lots of interest in PD research, there are also several other proteins that are present in the Lewy bodies such as ubiquitin and other proteasomal proteins pointing to a role of a failure of protein clearance systems in the pathophysiology of neurodegeneration. Protein accumulation and aggregation may be facilitated by disturbances in cellular clearance and processing pathways, such as ubiquitin-proteasome (UPS) and autophagy-lysosome systems (Ebrahimi-Fakhari et al. 2012). Importantly, UPS dysfunctions have been linked to PD; decreased proteasomal activity has been identified in the SNc of PD patients (McNaught and Jenner 2001; McNaught et al. 2003; Tofaris et al. 2003), and genetic mutations in an ubiquitin ligase, parkin, have been linked to early-onset Parkinsonism (Kitada et al. 1998). Various forms of aSyn have also been shown to compromise its own proteasomal clearance, thus promoting its accumulation (Snyder et al. 2003; Pan et al. 2008a; Ebrahimi-Fakhari et al. 2011). Furthermore, aSyn has been shown to inhibit proteasomal function (Ebrahimi-Fakhari et al. 2011) and A30P or A53T point mutated aSyn also inhibits chaperone-mediated autophagy (Cuervo et al. 2004), thus inducing their own accumulation and buildup of other proteins. It still remains to be clarified at what point of the aggregate formation process the protein clearance systems start to decline — at the onset or after protein already accumulates.

A more recent approach to model PD *in vivo* has been to use lactacystin (LC), a selective proteasome inhibitor (Fenteany and Schreiber 1998). It has been successfully used in rats and mice and it appears that the nigral administration produces a fast-onset PD-like phenotype, including aSyn accumulation, tyrosine hydroxylase (TH) positive cell loss and behavioral deficits (McNaught et al. 2002; Pan et al. 2008b; Lorenc-Koci et al. 2011; Bentea et al. 2015). Since ageing is one of the key predisposing factors to developing PD or other neurodegenerative diseases, we further characterized the nigral LC injection as a mouse PD model using young and adult mice. Furthermore, we wanted to study the neuroinflammatory responses in this model, because they have not been thoroughly investigated in previous models. We have also analysed the key elements of a PD model: motor behavior, dopamine cell loss, and aSyn accumulation after LC administration. In addition, to further characterizing the model, we studied the expression of gamma-Aminobutyric acid (GABA) markers since increase of GABAergic neurotransmission after the decrease in inhibitory dopaminergic neurons has been described in PD models (Salin et al. 2002; Wang et al. 2010)

Experimental procedures

Chemicals

Chemicals used were purchased from Sigma-Aldrich (St. Louis, MO, USA) unless otherwise specified. Ethanol was purchased from Altia (Helsinki, Finland). LC was purchased from A.G. Scientific (#L-1147; San Diego, CA, USA) and dissolved in PBS in concentration of 2 mg/ml. LC solution was protected from light.

Animals

Male C57Bl/6RccHsd mice were obtained from Harlan Laboratories. Mice that were 8-9 weeks (young) and 12-14 months (adult) old were used for the experiments The animals were maintained at 20-22 °C room temperature with 12:12 h light:dark rhythm and had *ad libitum* access to food and water. The experiments were carried out according to the European Community guidelines for the use of experimental animals and approved by the Finnish National Board of Animal Experiments (ESAVI/198/04.10.07/2014).

Stereotactic microinjection and drug treatments

The mice were deeply anaesthetized (Univentor anaesthesia unit, Zejtun, Malta) with 2-4 % isoflurane (Baxter, Deerfield, IL, USA) and placed on a stereotactic frame (Stoelting, Wood Dale, IL, US) for injection of 2 µg of LC above the SNc. A 1 µl injection of LC was delivered with a 10 µl –microsyringe (World Precision Instruments, Sarasota, FL, USA) connected to an injector (Quintessential stereotaxic injector, Stoelting) at 0.2 µl/min on the right side of the brain to the following coordinates: A/P -3.2; M/L -1.2 ; D/V -4.3 from the bregma according to (Franklin and Paxinos 1997), and the needle was left in place for 5 minutes after injection until it was slowly withdrawn. Mice received subcutaneous buprenorphine 0.05 mg/kg (Temgesic, Reckit Benckiser Healthcare Ltd, Slough, UK) for post-operative pain relief, and lidocaine (Orion Pharma, Espoo, Finland) was used as a local anesthetic during the operation. Number of animals injected was: Young mice n=10 LC injected and n=8 PBS injected (vehicle) for immunohistochemistry and behavioral analysis, and a separate cohort of n=7 for HPLC analysis; adult mice n=3 LC injected and n=4 vehicle injected. Since we wanted to characterize the fast-onset effects of LC injection, and a previous study (Bentea et al. 2015) reported the mice having the most disturbances in their motor behavior 1 week post-injection, the mice were

sacrificed on the 10th day post injection.

Cylinder test

The cylinder test to evaluate forelimb use asymmetry was performed as described previously (Schallert et al. 2000). More specifically, the mice were removed from their home cage and placed in a plexiglass cylinder (diameter 12 cm, height 15 cm) that rested on a clear plastic platform. A video camera was placed directly underneath the cylinder and each mouse was recorded for 5 min, and then returned to its home cage. Animals were scored by an observer blind to the treatments. The number of touches for each ipsilateral, contralateral, and simultaneous paw placement were recorded. The test was done on the 8th day after LC or PBS microinjection. The contralateral paw use preference was calculated using the following equation: (contralateral paw contacts + 0.5 x both paw contacts) / (ipsilateral + contralateral + both paw contacts). The number of animals was 8 in vehicle and 10 in LC group in young animals, and 4 in vehicle and 3 in LC group adult animals.

Horizontal and vertical activity

The horizontal and vertical activity was tested as described in (Mijatovic et al. 2007) to evaluate the effect of LC lesion on the spontaneous locomotor activity. Measurement was performed on the 9th day after injection. Mice were placed in transparent cages (25 cm × 25 cm × 15 cm) in the activity monitor measuring infrared beam interruptions (MED Associates, St. Albans, GA, USA). Due the short length of the experiment, no food or water was placed to cages. The measurement was started right after mice were placed in the cages and the data was collected at 15 min intervals for 2 h. The number of animals was 8 in vehicle and 10 in LC group in young animals, and 4 in vehicle and 3 in LC group adult animals.

Tissue dissection

On the 10th day after LC or PBS microinjection, mice were deeply anesthetized with sodium pentobarbital (150 mg/kg, i.p.) and transcardially perfused first with phosphate-buffered saline (PBS) to remove blood and then with 4 % paraformaldehyde (in PBS) to fix the tissue for immunohistochemistry. Brains were removed and immersed in 4 % paraformaldehyde overnight to fix the tissue. The brains were then immersed first in 10 % sucrose solution (in PBS) for overnight following with 30 % sucrose solution, kept in +4°C until they sank, after which the samples were quickly frozen with isopentane on dry ice and stored at -80 °C until

sectioning. Brains were sectioned at 30 µm thickness. Floating sections were stored in -20 °C. For high-pressure liquid chromatograph (HPLC), striatal samples were quickly dissected from fresh brain tissue after PBS perfusion and frozen at -80 °C until homogenization (described in Mijatovic et al. 2011).

Immunohistochemistry

For the analysis of brain aSyn, glutamic acid decarboxylase 65/67 (GAD), tyrosine hydroxylase (TH), and glial cell markers (glial fibrillary acidic protein; GFAP and ionized calcium-binding adapter molecule; Iba1), immunohistochemistry was performed as described in (Mijatovic et al. 2007; Myohanen et al. 2012). In brief, the endogenous peroxidase activity was inactivated with 10% methanol and 3% H_2O_2 in PBS (pH 7.4) for 10 min (not in immunofluorescence staining), and non-specific binding was blocked with 10% normal donkey serum (aSyn, Iba1) (#S30, Millipore, Temencula, CA, USA) or 10% normal goat serum (TH, GAD, GFAP, Iba1, Ubiquitin) (#S-1000, Vector Laboratories, Burlingame, CA, USA) or 10% normal rabbit serum (GFAP-IFL) (#S-5000, Vector Laboratories) in PBS containing 0.5 % Triton-X-100. The sections were incubated overnight at room temperature with primary antibodies in 1% normal serum in PBS (see details in Table 1) followed by washing with PBS. The sections were then incubated with the following secondary antibodies, depending on primary antibody; donkey anti-sheep HRP conjugated secondary antibody (aSyn) (1:500, #ab6900, Abcam), goat anti-rabbit HRP conjugated secondary antibody (GAD) (1:500, #31460, Thermo Scientific, Rockford, USA), goat anti-rabbit biotinylated secondary antibody (TH, GFAP and Iba1; 1:500, BA1000, Vector Laboratories), goat anti-rabbit Texas Red conjugated (ubiquitin) (1:200, #T-2767, Thermo Scientific), rabbit anti-chicken fluorescein conjugated (GFAP-IFL) (1:300, #31501, Thermo Scientific) or donkey anti-goat Alexa Fluor 488 conjugated (Iba1-IFL) antibodies (1:200, ab150129, Abcam). The signal for TH, GFAP and Iba1 staining was enhanced with the avidin-biotin complex –method (Vectastain® ABC kit standard, #PK-4000, Vector Laboratories). The antigen-antibody complexes were visualized following incubation with 0.05% 3,3'-diaminobenzidine and 0.03% hydrogen peroxide solution. Finally, the DAB-stained sections were moved to objective glass, dehydrated in alcohol series and mounted with Depex (BDH, Poole, UK). Fluorescently labeled sections were mounted with Vectashield (H-1200, Vector Laboratories)

Stereological counting and optical density analysis

The number of TH-positive neurons in the SNc was analyzed by a person blinded to the

treatment groups. Three sections from each animal were selected (every 6th section). StereoInvestigator (MBF Bioscience, USA) was used for the stereological analysis. TH-positive cells were counted at predetermined intervals (x = 100 µm, y = 80 µm) within the counting frame (60 µm × 60 µm) superimposed on the image using a 60× oil objective (Olympus BX51, Olympus Optical, Japan) equipped with an Optronics camera.

For optical density (OD) analysis of aSyn, TH and GAD, immunohistochemically stained brain sections were imaged using 3DHISTECH slide scanner (3DHISTECH Ltd., Budabest, Hungary) at the service provided in the Institute of Biotechnology, University of Helsinki. ODs were analysed using ImageJ (NIH, Bethesda, MD, USA). Images were converted into grayscale and inverted before analysis. Area to be analyzed was selected using the freehand selection – tool. The background staining values of each brain area were subtracted from raw data values of the same brain area.

Neuroinflammation in the brain was semi-quantitatively analyzed using Image Pro Plus 6 software (Media Cybernetics, Rockville, MD, USA). Briefly, images of brain sections that were exported from 3DHISTECH were converted into grayscale and inverted. Then pre-determined area was analyzed from the substantia nigra (SN) injection side and control side. To estimate area stained in the striatum, a circular annotation was drawn over the area and same sized regions were analyzed from both sides. Area stained in the selected regions were counted using count and measure objects tool.

Number of animals in aSyn, TH and GAD analysis was 4 in vehicle group and 8 in LC group (young) and 4 in vehicle and 3 in LC group (adult). In glial cell markers, the number of animals was 3 in vehicle and 3 in LC group in both age groups. Altogether 3-4 samples of each brain area/staining per animal per group were analyzed. OD values for each mouse were calculated as OD injection side / OD intact side x 100 %. Image panels were prepared by Adobe Photoshop CS6 software (version 13.0, Adobe Systems, San Jose, CA, USA).

Confocal microscopy

Fluorescent double-labeled sections were photographed using an upright microscope (Leica DM5000B, Leica Microsystems Inc.) with broadband laser confocal device (Leica TCS SP5, Leica Microsystems Inc.). After the images were captured with an imaging device, confocal double-labeled immunofluorescence micrographs were merged to detect colocalization by using Adobe Photoshop CS6 software (Adobe Systems). Only corrections to brightness and contrast were made.

Analysis of neurotransmitters and metabolites

The striatal brain tissue samples were homogenized as described earlier (Airavaara et al. 2006). Briefly, the striatal samples were homogenized in 0.5 ml of homogenization solution (0.2 M $HClO_4$ and antioxidant solution). The homogenates were centrifuged at 20,800g for 35 min at 4℃. Supernatant was removed to 0.5 ml Vivaspin filter concentrators (10,000 MWCO PES; Vivascience AG, Hannover, Germany) and centrifuged at 8,600g at 4℃ for 35 min. The tissue concentrations of dopamine, its main metabolites 3,4-dihydroxyphenylacetic acid (DOPAC) and homovanillic acid **(**HVA), and serotonin (5-HT) and its metabolite 5-hydroxyindoleacetic acid (5-HIAA) were analyzed with a HPLC equipped with an electrochemical detector. Concentrations are calculated as nanograms per milligram of brain tissue. Number of animals was 7 in both treatment groups.

Statistics

Statistical analysis was done using GraphPad Prism 5 and 6 softwares. Student's *t*-test, 1-way ANOVA with Newman-Keuls multiple comparisons or 2-way ANOVA with Tukey's multiple comparisons test were used. Data is presented as Mean ± SEM and F-values are included with statistics.

Results

Motor impairment after LC administration

To evaluate the degree of LC-induced unilateral lesion in the nigrostriatal tract we measured horizontal and vertical locomotor activity as well as assessed the ipsilateral and contralateral limb use with cylinder test in mice. Additionally, we observed spontaneous contralateral rotating behavior in LC-injected mice of both age groups starting and being the strongest 2 to 3 days after the injection and continuing to the end of the experiment but this was not quantitatively analyzed.

Cylinder test

The paw use preference during rearing was measured with cylinder test. LC groups had reduced use of contralateral paw 8 days after lesioning pointing to unilateral damage of nigrostriatal

tract (Fig 1E-F; $t = 2.751$, $df = 16$; P = 0.0142 and Adult: $t = 2.390$, $df = 5$; P = 0.0624, Student's *t*-test).

Horizontal and vertical activity

Locomotor activity was measured for 2 h on the 9th day after LC lesioning. LC showed a trend to reduce total distance travelled (Fig 1A; Young: $t = 1.776$; $df = 16$; P = 0.0948, Student's *t*-test) and vertical counts (Fig 1B; $t = 1.941$, $df = 16$; P = 0.0701, Student's *t*-test) in young mice. In adult animals, there were no alterations in distance travelled or vertical activity, although the trend in distance travelled was opposite to young mice (Fig. 1C-D; $t = 0.9442$, $df = 5$; P = 0.3884 and $t = 0.047$, $df = 5$; P = 0.9643 respectively, Student's *t*-test). However, the number of animals in adult mice groups (3 and 4) is not sufficient to achieve statistically reliable results in behavioral tests, and therefore, these results cannot be considered conclusive.

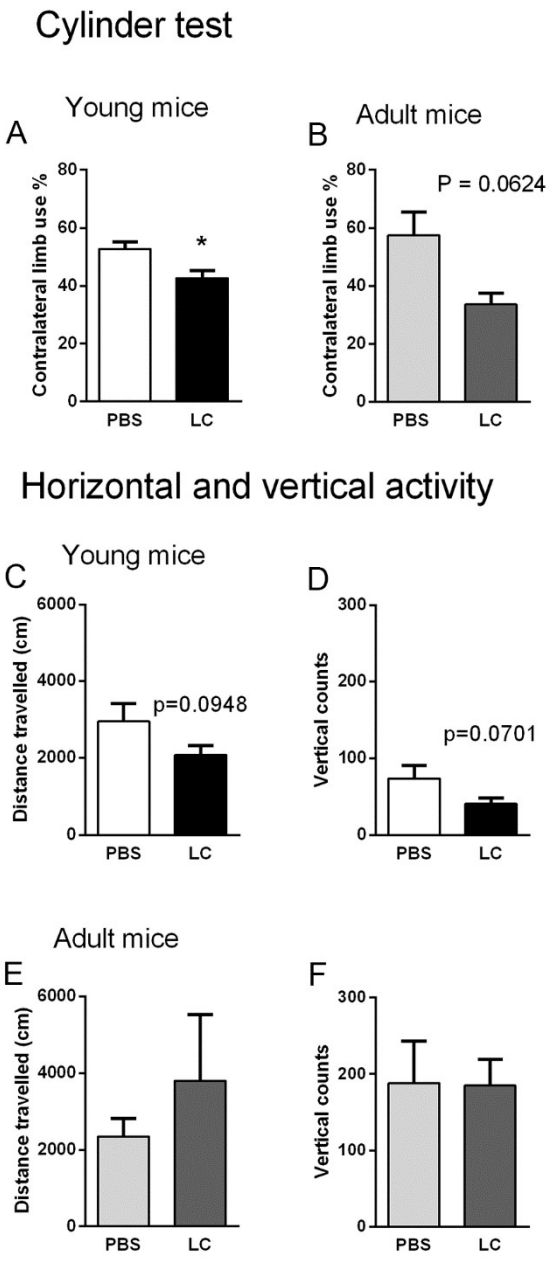

Fig. 1A-F: The behavioral assessment of mice after unilateral nigral lactacystin (LC) lesioning by cylinder and locomotor activity tests. The paw use preference for rearing 8 days after LC injection was measured by cylinder test. Both LC groups showed decreased use of contralateral paw (Young mice: P = 0.0142) although insignificantly in adult mice (ns, P = 0.0624) (A-B). Horizontal and vertical activity was measured for 2 h 9 days after LC (2 µg) injection. Stereotactic injection of PBS was used as a sham control. In young, 8-9 weeks old mice, LC shows a trend to decrease total distance travelled (ns, P = 0.0948) (C) and vertical counts (ns, P = 0.0701) (D). In adult mice, no effect was seen in the locomotor activity (E-F). * P < 0.05; unpaired Student's t-test was used as statistical analysis in all experiments; n=10 LC injected and 8 vehicle in young mice, n= 3 LC injected and 4 vehicle in adult mice.

Reduction of markers of nigrostriatal dopamine system after LC injection

In the SNc, LC induced approx. 40% TH-positive neuron loss in young mice and 50% decrease in adult mice (Fig 2D-F; Young: $t = 3.432$, $df = 10$; P = 0.0064; Fig 2J-L; Adult: $t = 2.358$, $df = 5$; P = 0.0649). TH positive neurons remaining in the LC-lesioned side compared to the unlesioned side of the SNc were 64.9 ± 5.4 % in the young and 62.6 ± 15.52 in the adult mice (Fig 2F and L). LC significantly decreased striatal TH OD (Fig 2A-C; Young: $t = 4.412$, $df = 9$; P = 0.0017; Fig 2G-H; Adult: $t = 3.620$, $df = 5$; P = 0.0152, Student's *t*-test) and TH loss was significantly greater in the adult mice; the remaining amount of TH-positive terminals in the lesion side compared to control side was 61.39 ±10.7 % in adult and 80.1 ± 2.8 % in young mice (Fig 2C and I). This was also observed in 2-way ANOVA analysis (Fig. 2M) where LC had a significant effect on striatal TH (P<0.0001; F(1,14) = 33.76, 2-way ANOVA) and there was also an interaction with the age of the mice (P = 0.0432; F(1,14) = 4.944, interaction (LC*age), 2-way ANOVA).

Striatal dopamine levels were measured only from the young mice after LC lesion. LC injection above the SN decreased the level of striatal dopamine by approximately 55 % (Fig 2N; $t = 3.581$, $df = 12$; P = 0.0038) and its metabolite DOPAC (Fig 2N; $t = 2.737$, $df = 12$; P = 0.0180) compared to intact side. The levels of HVA were not significantly altered (Fig 2N; $t = 0.5983$, $df = 12$; P = 0.5608). LC did not affect 5-HT or 5-HIAA levels (See supplementary materials S1).

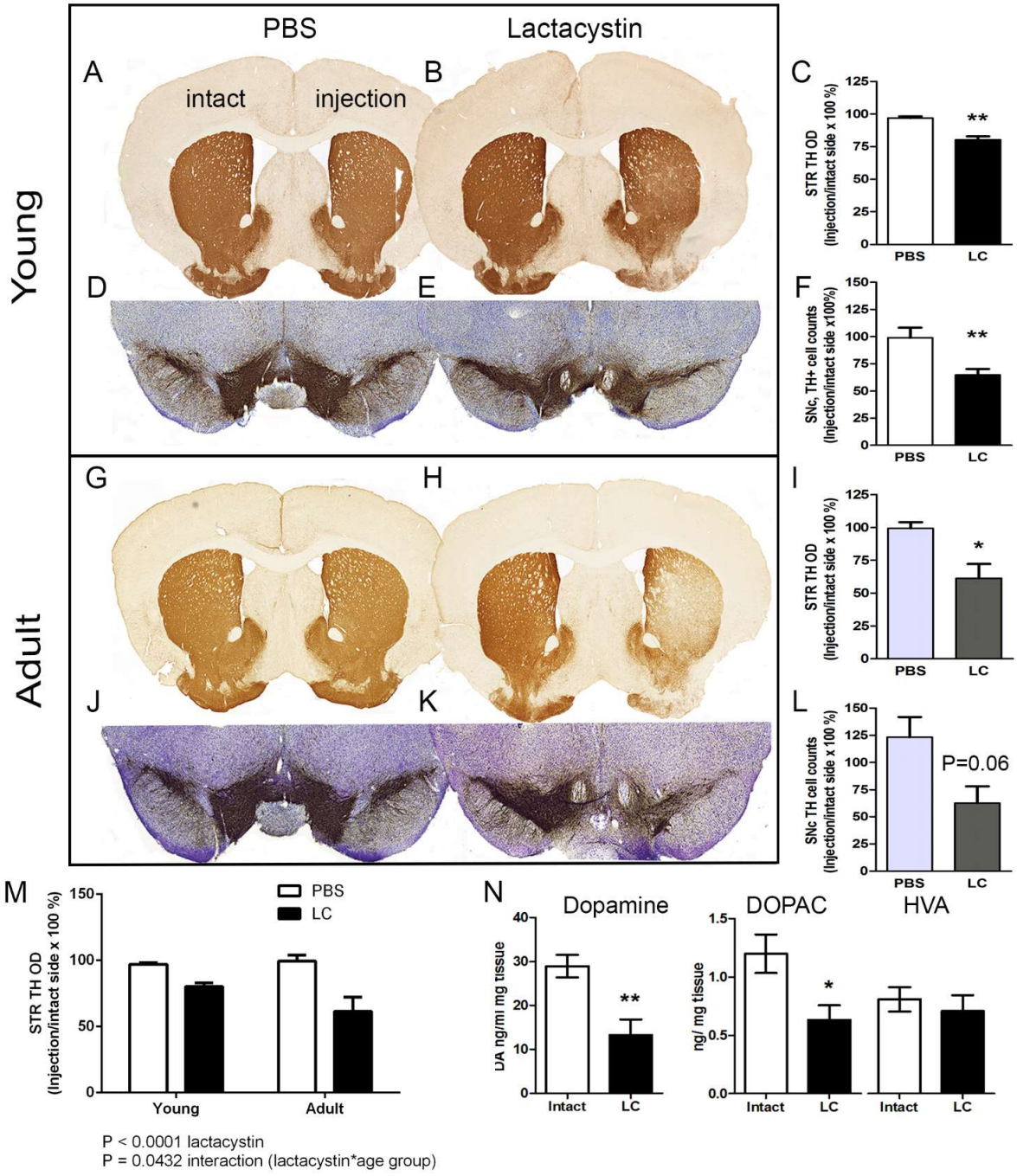

Fig. 2A-M. Tyrosine hydroxylase (TH) positive neuron loss and reduced striatal dopamine (DA) and metabolite content after lactacystin (LC) lesion. LC administered supranigrally significantly decreased TH optical density (OD) in the striatum of young (8-9 weeks old, A-C), and in the striatum of adult mice (12-14 months old, G-I). The interaction between striatal TH decrease and age and LC injection was also observed in 2-way ANOVA analysis (M; P<0.0001 LC; P = 0.0432 interaction (age*LC), 2-way ANOVA). In the substantia nigra pars compacta (SNc) the cell loss was at the same level in both age groups (Young D-F; Adult J-L, P = 0.06 in adult mice). In the young mice, 10 days after LC injection significant depletion of the striatal DA (N) and 3,4-dihydroxyphenylacetic acid (DOPAC) levels were observed. However, no significant decrease was seen in the homovanillic acid (HVA) levels. * P < 0.05, ** P < 0.01; unpaired Student's t-test was used as statistical analysis in all experiments; n=8 LC injected

and 4 vehicle in young mice, n=3 LC injected and 4 vehicle in adult mice; n=7 in both groups in HPLC assays.

LC-induced glial cell activation and accumulation of ubiquitinated proteins in glial cells

Lactacystin induced strong and widespread astroglial cell activation. Intense GFAP immunoreactivity was seen throughout the whole injected hemisphere at the SN level (anterior-posterior) after lactacystin injection compared to PBS and to uninjected side (Fig 3A-B, Q, $P = 0.0003$; $F(3,11) = 23.20$, $P<0.001$ Newman-Keuls post-hoc test, 1-way ANOVA). Lactacystin also increased the expression of ubiquitinated proteins in GFAP positive cells that was not seen in such high amounts in the control side (Fig. 4A-L) or after PBS injection (Supplementary Fig. S2). Although we saw an increased GFAP activation around the lactacystin-injected brain hemisphere in adult mice (Fig. 3C-D), due to large variance in our small sample group the data did not reach significance in the statistical assay. Moreover, astroglial activation was also seen in the striatum, particularly in adult mice (Fig 3E-F, R; Young: lactacystin vs. PBS; $P = 0.0150$; $F(3,11) = 6.563$, $P<0.01$, intact vs lactacystin; $P<0.05$; Adult: lactacystin vs. PBS; $P = 0.0054$; $F(3,11) = 9.378$, $P<0.01$ Newman-Keuls post-hoc test, 1-way ANOVA) but not in the cortical brain structures of the injected side.

In addition to astroglial activation, microglial cells detected by Iba1 were intensively activated in the SN level after LC injection (Fig 3I-J, S; Young: intact vs LC; $P = 0.0002$; $F(1,8)=39.88$, $P<0.01$; Fig 3K-L, V; Adult: LC vs. PBS $P = 0.0014$ $F(1,8)=22.56$, $P<0.01$, intact vs LC $P = 0.0092$; $F(1,8)=11.64$, $P<0.01$ Tukey's post-hoc test, 2-way ANOVA). Similar to astroglial cells, microglial cell activation was widespread, covering the whole LC-injected brain hemisphere at the level of injection (anterior-posterior) in both young and adult mice (Fig 3M-P). In addition, similar accumulation of ubiquitinated proteins as in GFAP positive astroglial cells were seen in microglial cells in double-label immunofluorescence (Fig. 4M-X). No difference in activation of microglial cells was observed in the striatum.

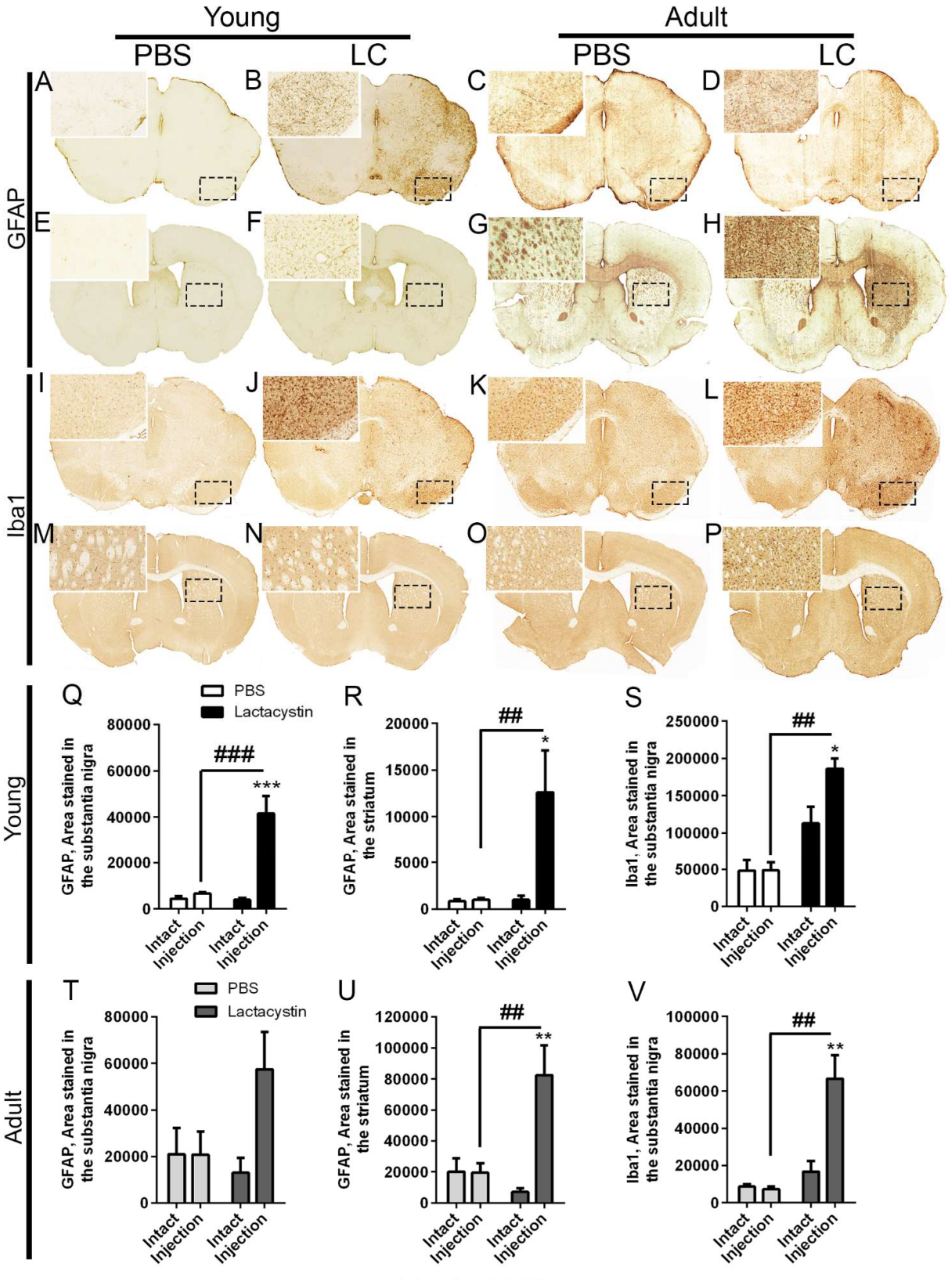

Fig. 3A-V. The effects of lactacystin (LC) on GFAP and Iba1 immunoreactivity. LC microinjection above the substantia nigra induced widespread activation of astroglial cells around the hemisphere of injection side at nigral level, that were detected by glial fibrillary acidic protein (GFAP) staining (Young, A-B, Q; Adult, C-D, T). GFAP immunostaining was also seen in the striatum after LC injection and it was particularly intense in adult mice (Young, E-F, R; Adult, G-H, U). Similar to GFAP, microglial cells were significantly activated in LC

injected side (ionized calcium-binding adapter molecule (Iba1); Young, I-J, M-N, S; Adult, K-L, O-P, V). Young mice 8-9 weeks old, Adult mice 12-14 months old. Scale bar is 100 µm. * P < 0.05, ** P < 0.01, P < 0.001, vs. intact, # P < 0.05, ## P< 0.01, ### P < 0.001 vs. PBS injection; GFAP: Newman-Keuls post-hoc test, 1-way ANOVA; Iba1: Tukeys's post-hoc test, 2-way ANOVA; n=3 in all groups.

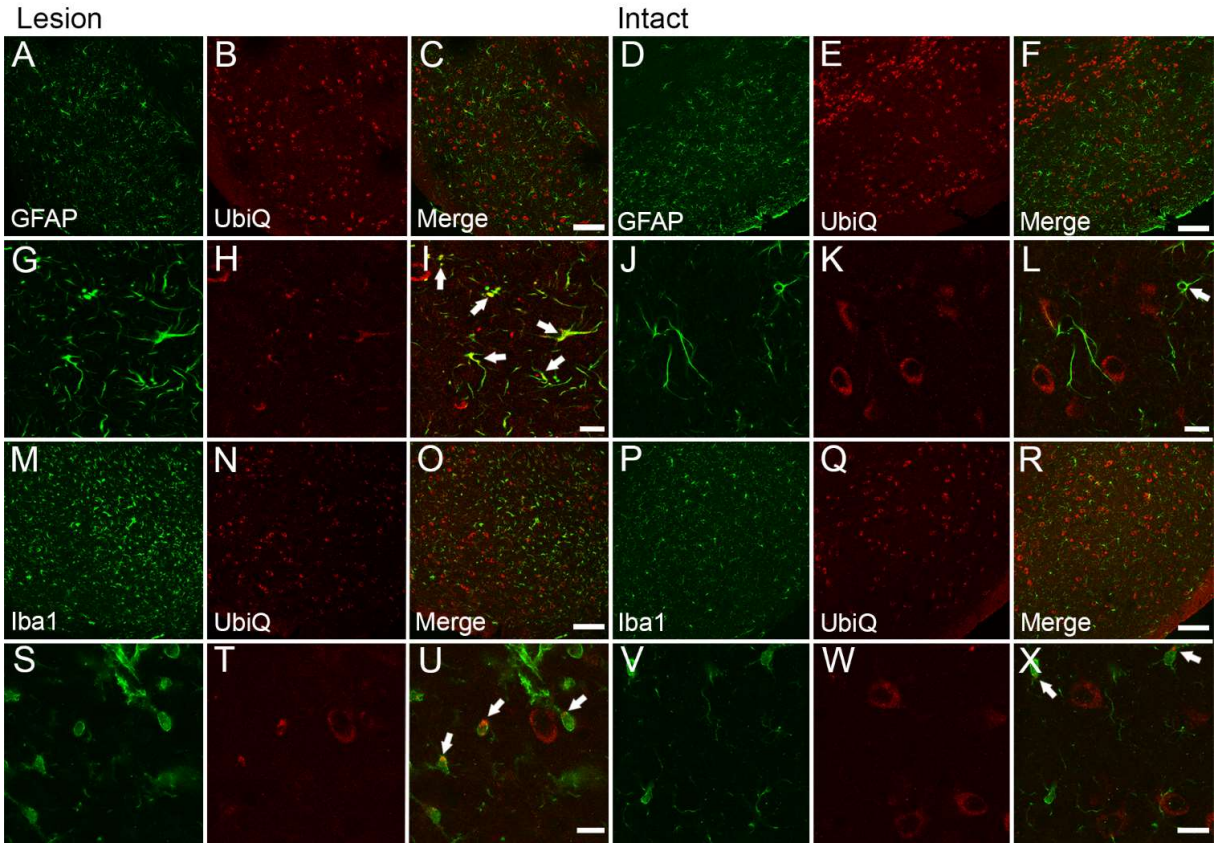

Fig. 4A-X. Accumulation of ubiquitin-labelled proteins in astroglial and microglial cells after lactacystin injection. Ubiquitin-immunostained (UbiQ) cells were generally decreased in LC injected side of the substantia nigra (B, N) compared to intact side (E, Q). Increased colocalization between UbiQ and GFAP was seen after LC injection (G-I), and similar staining was seen between UbiQ and Iba1 (S-U). In intact side, less colocalization was seen with UbiQ both in GFAP and Iba1-labelled cells (J-L, V-X). White arrows are pointing to the colocalization. Scale bar is 50 µm in A-F and M-R, and 5 µm in G-L and S-X.

LC induces aSyn accumulation in the substantia nigra

LC produced robust accumulation of aSyn in the SN compared to PBS control group (Fig 5A-C and E-G; Young: $df = 14$; P = 0.0012; Adult: $t = 3.161$, $df = 5$; P = 0.0251, Student's t-test). Accumulation percentages for young mice are 105.4 ± 5.1 for PBS, 169.3 ± 20 for LC and for adult mice 104.8 ± 16.9 vs. 185.7 ± 19.2 (Fig 5C and G). The accumulation was observed both in the SNc and SN pars reticulata (SNr). We did not observe a significant increase of aSyn in the striatum after LC (Fig 5D and H).

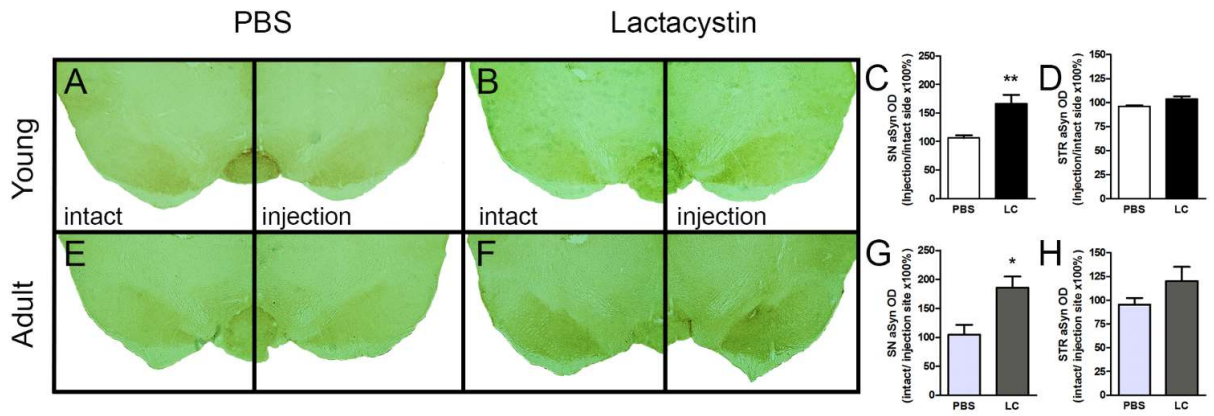

Fig. 5A-H. Accumulation of α-synuclein (aSyn) in SN after lactacystin (LC) injection. Representative images of nigral aSyn immunostaining 10 days after nigral stereotaxic injection of PBS and LC in young (A-B) and adult (E-F) mouse. LC produced robust accumulation of aSyn in the substantia nigra (SN) compared to PBS control group (young mouse; C, $P < 0.01$; adult mouse; G, $P < 0.05$) However, significant accumulation of aSyn in the striatum was not detected in both groups (D, H). * $P < 0.05$, ** $P < 0.01$, unpaired Student's t-test; n=8 LC injected and 8 vehicle in young mice, n=3 LC injected and 4 vehicle in adult mice.

LC induces increase in GAD in SNr

As we observed aSyn accumulation in the SNr, we also wanted to study the expression of GAD, a GABA synthesising enzyme. We saw accumulation of GAD in the SNr after LC lesioning in young mice 142.3 ± 6.6 % compared to PBS control 103.8 ± 2.1 % and in adult mice 150 ± 8.5 % compared to 98.5 ± 5.9 % (Fig 6A-C, Young: $t = 5.094$, $df = 14$; $P = 0.0001$; D-F, Adult: $t = 5.180$, $df = 5$; $P = 0.0035$; Student's t-test).

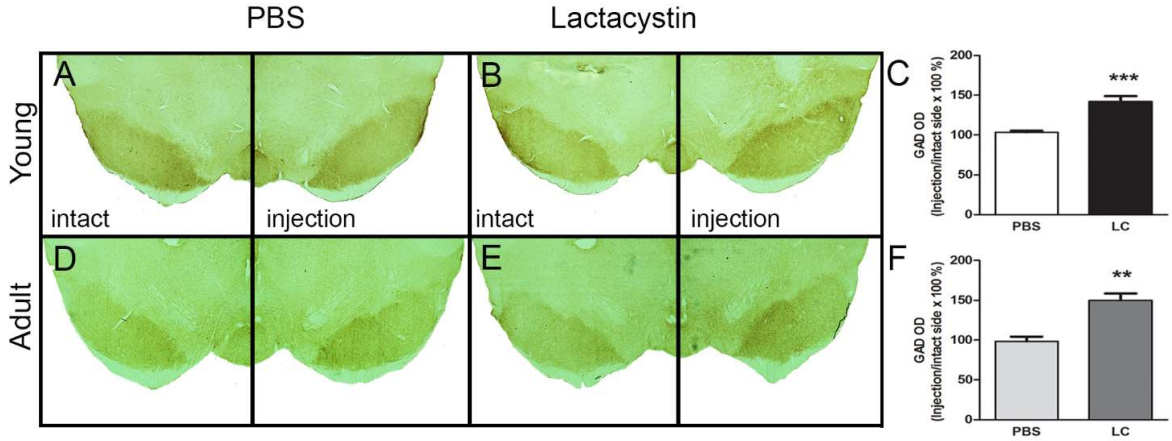

Fig. 6A-F. Accumulation of glutamic acid decarboxylase 65/67 (GAD) in the SN pars reticulata (SNr) after lactacystin (LC) lesioning. In both age groups (Young 8-9 weeks old (A-C), adult 12-14 months old (D-F)) significant accumulation GABA synthesising enzyme, GAD, was observed compared to sham lesion control (young mouse; C, $P < 0.001$; adult mouse; F, $P < 0.01$). ** $P < 0.01$, *** $P < 0.001$, unpaired Student's t-test; n=8 LC injected and 8 vehicle in young mice, n=3 LC injected and 4 vehicle in adult mice.

Discussion

In this study, we have characterized a mouse model of PD that is based on direct proteasomal inhibition in the SN of young and adult mice. Although LC has been used as a PD model in earlier studies either by injecting it into the medial forebrain bundle or striatum (Fornai et al. 2003; Vernon et al. 2011; Shen et al. 2013; Konieczny et al. 2014a), and recently in mouse (Bentea et al. 2015; Kumar et al. 2015) and rat (Konieczny et al. 2014b; Harrison et al. 2015; Pienaar et al. 2015) SN, to our knowledge this is the first time when LC injection has also been used in adult mice and wide-spread neuroinflammation has been observed and thoroughly analyzed. The model shows several well-established features of PD – motor deficits, nigrostriatal dopamine loss and aSyn accumulation as the most important, and we indeed detected differences in response between young and adult mice. However, the number of adult mice in the current study was low and this should be kept in mind when drawing conclusions based on our results.

Young LC-injected mice showed hypolocomotion in 2 h locomotor activity test and both age groups had a tendency to use more ipsilateral paw in cylinder test, indicating a deficit of nigrostriatal dopaminergic system. In mice, LC injection in medial forebrain bundle (MFB) or SN has been shown to rapidly induce motor behavioral decline (Li et al. 2010; Bentea et al. 2015), and similarly in rats, motor decline has been reported after MFB or SN injection (Vernon et al. 2011; Konieczny et al. 2014a). Interestingly, striatal injection of LC in rats did not cause behavioral decline in a study by (Lorenc-Koci et al. 2011).

LC rapidly produced dopaminergic neurodegeneration in SN and depletion of striatal dopamine levels leading to motor behavioral deficits, which is an important aspect for a PD model. Our observations are similar to previous studies (Vernon et al. 2011; Bentea et al. 2015) which showed the maximal neurodegenerative effect of LC at one week after injection. In our study, significant TH positive cell loss was observed in SNc, but in our 10-day study the lesion did not markedly proceed to the striatum in the young mice when TH positive terminals were analysed. However, striatal dopamine and DOPAC levels were reduced by 55%, suggesting that dopamine synthesis is decreased although the TH protein is still present. This may suggest that TH has been inhibited or neuronal damage is still progressing at day 10, although in another study striatal dopamine and DOPAC levels did not decrease any further after 1 week (Bentea et al. 2015). However, the dose of LC may explain this difference; Bentea et al. used a 3 µg dose in mice, whereas in our studies the dose was 2 µg, and it is possible that with a lower dose the neuronal degeneration is still progressing. Slow progression of LC-induced pathology has

also been reported by Harrison et al. (2016) where they noticed a decrease in TH positive neurons of the ventral tegmental area 5 weeks after LC injection. Moreover, aSyn is known to inhibit TH activity (Perez et al. 2002; Lou et al. 2010), and we observed increased aSyn levels in the SN, suggesting a mechanism for reduced dopamine content in the striatum. When we investigated striatal TH ODs in young and adult mice, the TH loss seems to be greater in the adult mice, which supports the role of age as a factor for neurodegeneration. Although the number of adult mice was low in our study, the results suggest that it might increase the validity and translation of the results where the pre-clinical studies would be made in age-matched animals. Dopaminergic neurotransmission inhibits the GABAergic system, and when dopaminergic regulation is decreased in PD, GABAergic neurotransmission is enhanced (for review, see Galvan and Wichmann 2007). As presumed, in our study GAD expression was elevated in SNr, possibly contributing to a decrease of striatal dopamine. Increased GAD expression is also seen in earlier neurotoxin studies, where increased GABAergic activity (Wang et al. 2010) and GAD mRNA expression (Salin et al. 2002; Wang et al. 2010) in the lesion side in PD 6-OHDA rat model has been reported. In addition, LC is not a specific toxin for dopaminergic neurons, and increase in GAD may also propose that dopaminergic neurons are more sensitive for LC toxicity than GABAergic neurons in SN.

Interestingly, we observed massive glial cell activation after LC injection. Glial activation is characteristic for PD and other synucleinopathies (McGeer et al. 1988; Gerhard et al. 2003; Braak et al. 2007; Stefanova et al. 2007; Iannaccone et al. 2013). Both astroglial and microglial cells were activated throughout the LC injected hemisphere and this indicates that LC, and possibly also increased aSyn protein accumulation, have activated a pro-inflammatory signal cascade leading to widespread activation of glial cells that may further enhance the neurodegeneration (Imamura et al. 2003; Gao et al. 2008; Kwon et al. 2008; Lee et al. 2010). Glial activation in the SN in the LC model has earlier been reported in mice (Li et al. 2010) but in the rat model no remarkable activation three weeks after injection was seen (McNaught et al. 2002). However, in the studies by Pienaar et al. (2015) and Elson et al. (2016), LC injection to rat SN caused significantly increased microglial cell activation in pedunculopontine nucleus that was accompanied by increased aSyn expression, supporting the spreading of aSyn pathology and glial activation after proteasome inhibition.

Proteasome inhibition has been shown to inhibit GFAP expression (Middeldorp et al. 2009) and despite the widespread astrogliosis, we saw reduced GFAP-immunostaining around the injection site in the SN indicating that astrogliosis is a result of activated inflammatory

cascades, not only spread of the 1 ul volume. Unfortunately, we are not able to directly compare a difference in the amount of activation of neuroinflammation in the two age groups of mice because they were not stained and sections were not scanned simultaneously. However, based on immunostaining, more intense spreading of astrogliosis to striatum was seen in adult mice, suggesting that their nigrostriatal tract is more vulnerable for glial activation. In addition to glial activation, we also detected increased ubiquitin-positive immunostaining in astroglial and microglial cells after LC injection. Astroglial cells are also responsive for proteasomal deficits and develop protein aggregates but they are not as sensitive as neurons (Goldbaum et al. 2009) and usually protein aggregates are less abundant than in neurons (Wakabayashi et al. 2000; Braak et al. 2007). However, proteasomal inhibition can disrupt glial cells (Kwon et al. 2008; Middeldorp et al. 2009) leading to their dysfunction that further enhances neurodegeneration. aSyn can also be directly transferred from neurons to astroglia which leads to formation of inclusion bodies and activation of microglia by cytokines and chemokines (Lee et al. 2010). Our results further support this finding.

Important for mimicking PD pathology, we observed increased aSyn immunostaining in the SN, supporting the role of proteasomes in aSyn accumulation and also the toxicity of aSyn to dopaminergic neurons. Recent studies have shown accumulation of phosphorylated aSyn in mice SN after LC injection (Bentea et al. 2015) in immunohistochemistry but also reduced soluble aSyn has been observed in rat (Lorenc-Koci et al. 2011) in Western blot. Although Lorenc-Koci et al (2011) did not measure the oligomeric forms of aSyn, the toxic species, it is likely that disturbed degradation of aSyn by blocking the proteasomes lead to increased concentration of aSyn which is a key factor to enhance the interaction between aSyn molecules, leading to aggregation of aSyn (Wood 1999). It remains a challenge to study aSyn protein aggregation in a mouse that does not have transgenic human aSyn, since there is a lack of decent and specific antibodies against mouse oligomeric or phosphorylated aSyn.

Conclusions

In this study we characterized various aspects of LC administration as a preclinical PD model and focused on studying the early changes (less than two weeks) occurring after injection. The presented LC mouse model very well establishes PD-like characteristics with motor disturbances, degeneration of TH positive neurons with dopamine loss, aSyn accumulation and neuroinflammation. In addition, although the number of adult mice in this study was low, our

results suggest that older mice were more sensitive for dopaminergic cell loss compared to young animals, supporting their use in the PD toxin models. In longer-term studies, it might be rational to scale down the dose to observe a milder and progressive phenotype and to study the effects in human aSyn expressing/overexpressing animals. Furthermore, it remains to be studied what would be the long-term effects of LC in terms of aSyn aggregate formation and possible recovery. This model is an interesting pre-clinical tool to be used for studying many types of treatment strategies against PD and also other diseases associated with protein clearance deficits and neuronal inflammation.

Acknowledgements

Authors would like to thank Susanna Norrbacka, Kati Rautio and Liisa Lappalainen for excellent technical assistance. This work was supported by grants from the Academy of Finland (267788 and 2737991 (TTM) and 250275 (MA)), FinPharma Doctoral Programme (MS), Finnish Cultural Foundation (KA), the University of Helsinki grants (TTM), the Jane and Aatos Erkko Foundation (TTM.), the Sigrid Juselius Foundation (TTM), and the Emil Aaltonen Foundation (MS).

Conflicts of interests

Authors have no conflicts of interest to declare.

Ethical approval

All applicable international, national, and/or institutional guidelines for the care and use of animals were followed, and the use of experimental animals was approved by the Finnish National Board of Animal Experiments (ESAVI/198/04.10.07/2014).

References

Airavaara M, Mijatovic J, Vihavainen T, et al (2006) In heterozygous GDNF knockout mice the response of striatal dopaminergic system to acute morphine is altered. Synapse 59:321–329.

Bentea E, Van der Perren A, Van Liefferinge J, et al (2015) Nigral proteasome inhibition in mice leads to motor and non-motor deficits and increased expression of Ser129 phosphorylated alpha-synuclein. Front Behav Neurosci 9:68.

Braak H, Sastre M, Del Tredici K (2007) Development of alpha-synuclein immunoreactive astrocytes in the forebrain parallels stages of intraneuronal pathology in sporadic Parkinson's disease. Acta

Neuropathol 114:231–241.

Cuervo AM, Stefanis L, Fredenburg R, et al (2004) Impaired degradation of mutant alpha-synuclein by chaperone-mediated autophagy. Science 305:1292–1295.

Decressac M, Mattsson B, Lundblad M, et al (2012) Progressive neurodegenerative and behavioural changes induced by AAV-mediated overexpression of alpha-synuclein in midbrain dopamine neurons. Neurobiol Dis 45:939–953.

Ebrahimi-Fakhari D, Cantuti-Castelvetri I, Fan Z, et al (2011) Distinct roles in vivo for the ubiquitin-proteasome system and the autophagy-lysosomal pathway in the degradation of alpha-synuclein. J Neurosci 31:14508–14520.

Ebrahimi-Fakhari D, McLean PJ, Unni VK (2012) Alpha-synuclein's degradation in vivo: opening a new (cranial) window on the roles of degradation pathways in Parkinson disease. Autophagy 8:281–283.

Elson JL, Yates A, Pienaar IS (2016) Pedunculopontine cell loss and protein aggregation direct microglia activation in parkinsonian rats. Brain Struct Funct 221:2319–2341.

Fares M-B, Maco B, Oueslati A, et al (2016) Induction of de novo α-synuclein fibrillization in a neuronal model for Parkinson's disease. Proceedings of the National Academy of Sciences 113:E912–E921.

Fenteany G, Schreiber SL (1998) Lactacystin, proteasome function, and cell fate. J BiolChem 273:8545–8548.

Fornai F, Lenzi P, Gesi M, et al (2003) Fine structure and biochemical mechanisms underlying nigrostriatal inclusions and cell death after proteasome inhibition. JNeurosci 23:8955–8966.

Fornai F, Schlüter OM, Lenzi P, et al (2005) Parkinson-like syndrome induced by continuous MPTP infusion: convergent roles of the ubiquitin-proteasome system and alpha-synuclein. Proc Natl Acad Sci U S A 102:3413–3418.

Franklin K, Paxinos G (1997) The mouse brain in stereotaxic coordinates. Academic Press, San Diego, CA, USA

Galvan A, Wichmann T (2007) GABAergic circuits in the basal ganglia and movement disorders. Prog Brain Res 160:287–312.

Gao HM, Kotzbauer PT, Uryu K, et al (2008) Neuroinflammation and oxidation/nitration of alpha-synuclein linked to dopaminergic neurodegeneration. J Neurosci 28:7687–7698.

Gerhard A, Banati RB, Goerres GB, et al (2003) [11C](R)-PK11195 PET imaging of microglial activation in multiple system atrophy. Neurology 61:686–689.

Goldbaum O, Riedel M, Stahnke T, Richter-Landsberg C (2009) The small heat shock protein HSP25 protects astrocytes against stress induced by proteasomal inhibition. Glia 57:1566–1577.

Harrison IF, Anis HK, Dexter DT (2016) Associated degeneration of ventral tegmental area dopaminergic neurons in the rat nigrostriatal lactacystin model of parkinsonism and their neuroprotection by valproate. Neurosci Lett 614:16–23.

Harrison IF, Crum WR, Vernon AC, Dexter DT (2015) Neurorestoration induced by the HDAC inhibitor sodium valproate in the lactacystin model of Parkinson's is associated with histone acetylation and up-regulation of neurotrophic factors. Br J Pharmacol 172:4200–4215.

Iannaccone S, Cerami C, Alessio M, et al (2013) In vivo microglia activation in very early dementia

with Lewy bodies, comparison with Parkinson's disease. Parkinsonism Relat Disord 19:47–52.

Imamura K, Hishikawa N, Sawada M, et al (2003) Distribution of major histocompatibility complex class II-positive microglia and cytokine profile of Parkinson's disease brains. Acta Neuropathol 106:518–526.

Jin J, Meredith GE, Chen L, et al (2005) Quantitative proteomic analysis of mitochondrial proteins: relevance to Lewy body formation and Parkinson's disease. Brain Res Mol Brain Res 134:119–138.

Kahle PJ, Neumann M, Ozmen L, et al (2001) Selective insolubility of alpha-synuclein in human Lewy body diseases is recapitulated in a transgenic mouse model. Am J Pathol 159:2215–2225.

Kitada T, Asakawa S, Hattori N, et al (1998) Mutations in the parkin gene cause autosomal recessive juvenile parkinsonism. Nature 392:605–608.

Konieczny J, Czarnecka A, Lenda T, et al (2014a) Chronic L-DOPA treatment attenuates behavioral and biochemical deficits induced by unilateral lactacystin administration into the rat substantia nigra. Behav Brain Res 261:79–88.

Konieczny J, Jantas D, Lenda T, et al (2014b) Lack of neuroprotective effect of celastrol under conditions of proteasome inhibition by lactacystin in in vitro and in vivo studies: implications for Parkinson's disease. Neurotox Res 26:255–273.

Kumar A, Kopra J, Varendi K, et al (2015) GDNF Overexpression from the Native Locus Reveals its Role in the Nigrostriatal Dopaminergic System Function. PLoS Genet 11:e1005710.

Kwon SJ, Ahn TB, Yoon MY, Jeon BS (2008) BV-2 stimulation by lactacystin results in a strong inflammatory reaction and apoptotic neuronal death in SH-SY5Y cells. Brain Res 1205:116–121.

Lee HJ, Suk JE, Patrick C, et al (2010) Direct transfer of alpha-synuclein from neuron to astroglia causes inflammatory responses in synucleinopathies. J Biol Chem 285:9262–9272.

Li C, Guo Y, Xie W, et al (2010) Neuroprotection of pramipexole in UPS impairment induced animal model of Parkinson's disease. Neurochem Res 35:1546–1556.

Lorenc-Koci E, Lenda T, Antkiewicz-Michaluk L, et al (2011) Different effects of intranigral and intrastriatal administration of the proteasome inhibitor lactacystin on typical neurochemical and histological markers of Parkinson's disease in rats. Neurochem Int 58:839–849.

Lou H, Montoya SE, Alerte TN, et al (2010) Serine 129 phosphorylation reduces the ability of alpha-synuclein to regulate tyrosine hydroxylase and protein phosphatase 2A in vitro and in vivo. J Biol Chem 285:17648–17661.

Matsuoka Y, Vila M, Lincoln S, et al (2001) Lack of nigral pathology in transgenic mice expressing human alpha-synuclein driven by the tyrosine hydroxylase promoter. Neurobiol Dis 8:535–539.

McGeer PL, Itagaki S, Boyes BE, McGeer EG (1988) Reactive microglia are positive for HLA-DR in the substantia nigra of Parkinson's and Alzheimer's disease brains. Neurology 38:1285–1291.

McNaught KS, Belizaire R, Isacson O, et al (2003) Altered proteasomal function in sporadic Parkinson's disease. Exp Neurol 179:38–46.

McNaught KS, Bjorklund LM, Belizaire R, et al (2002) Proteasome inhibition causes nigral degeneration with inclusion bodies in rats. Neuroreport 13:1437–1441.

McNaught KS, Jenner P (2001) Proteasomal function is impaired in substantia nigra in Parkinson's disease. Neurosci Lett 297:191–194.

Meredith GE, Totterdell S, Petroske E, et al (2002) Lysosomal malfunction accompanies alpha-synuclein aggregation in a progressive mouse model of Parkinson's disease. Brain Res 956:156–165.

Middeldorp J, Kamphuis W, Sluijs JA, et al (2009) Intermediate filament transcription in astrocytes is repressed by proteasome inhibition. The FASEB Journal 23:2710–2726.

Mijatovic J, Airavaara M, Planken A, et al (2007) Constitutive Ret activity in knock-in multiple endocrine neoplasia type B mice induces profound elevation of brain dopamine concentration via enhanced synthesis and increases the number of TH-positive cells in the substantia nigra. J Neurosci 27:4799–4809.

Mijatovic J, Piltonen M, Alberton P, et al (2011) Constitutive Ret signaling is protective for dopaminergic cell bodies but not for axonal terminals. Neurobiol Aging 32:1486–1494.

Myohanen TT, Hannula MJ, Van Elzen R, et al (2012) A prolyl oligopeptidase inhibitor, KYP-2047, reduces alpha-synuclein protein levels and aggregates in cellular and animal models of Parkinson's disease. Br J Pharmacol. 166:1097-113

Pan T, Kondo S, Le W, Jankovic J (2008a) The role of autophagy-lysosome pathway in neurodegeneration associated with Parkinson's disease. Brain 131:1969–1978.

Pan T, Kondo S, Zhu W, et al (2008b) Neuroprotection of rapamycin in lactacystin-induced neurodegeneration via autophagy enhancement. Neurobiol Dis 32:16–25.

Perez RG, Waymire JC, Lin E, et al (2002) A role for alpha-synuclein in the regulation of dopamine biosynthesis. J Neurosci 22:3090–3099.

Pienaar IS, Harrison IF, Elson JL, et al (2015) An animal model mimicking pedunculopontine nucleus cholinergic degeneration in Parkinson's disease. Brain Struct Funct 220:479–500.

Salin P, Manrique C, Forni C, Kerkerian-Le Goff L (2002) High-frequency stimulation of the subthalamic nucleus selectively reverses dopamine denervation-induced cellular defects in the output structures of the basal ganglia in the rat. J Neurosci 22:5137–5148.

Schallert T, Fleming SM, Leasure JL, et al (2000) CNS plasticity and assessment of forelimb sensorimotor outcome in unilateral rat models of stroke, cortical ablation, parkinsonism and spinal cord injury. Neuropharmacology 39:777–787.

Shen YF, Tang Y, Zhang XJ, et al (2013) Adaptive changes in autophagy after UPS impairment in Parkinson's disease. Acta Pharmacol Sin 34:667–673.

Snyder H, Mensah K, Theisler C, et al (2003) Aggregated and monomeric alpha-synuclein bind to the S6' proteasomal protein and inhibit proteasomal function. J Biol Chem 278:11753–11759.

Spillantini MG, Crowther RA, Jakes R, et al (1998) alpha]-synuclein in filamentous inclusions of Lewy bodies from Parkinson's disease and dementia with Lewy bodies. Proc Natl Acad Sci U S A 95:6469–6473.

Stefanova N, Reindl M, Neumann M, et al (2007) Microglial activation mediates neurodegeneration related to oligodendroglial alpha-synucleinopathy: implications for multiple system atrophy. Mov Disord 22:2196–2203.

St Martin JL, Klucken J, Outeiro TF, et al (2007) Dopaminergic neuron loss and up-regulation of chaperone protein mRNA induced by targeted over-expression of alpha-synuclein in mouse substantia nigra. J Neurochem 100:1449–1457.

Tofaris GK, Garcia Reitbock P, Humby T, et al (2006) Pathological changes in dopaminergic nerve

cells of the substantia nigra and olfactory bulb in mice transgenic for truncated human alpha-synuclein(1-120): implications for Lewy body disorders. J Neurosci 26:3942–3950.

Tofaris GK, Razzaq A, Ghetti B, et al (2003) Ubiquitination of alpha-synuclein in Lewy bodies is a pathological event not associated with impairment of proteasome function. J Biol Chem 278:44405–44411.

Ulusoy A, Decressac M, Kirik D, Björklund A (2010) Viral vector-mediated overexpression of α-synuclein as a progressive model of Parkinson's disease. Prog Brain Res 184:89–111.

Vernon AC, Crum WR, Johansson SM, Modo M (2011) Evolution of extra-nigral damage predicts behavioural deficits in a rat proteasome inhibitor model of Parkinson's disease. PLoS One 6:e17269.

Wakabayashi K, Hayashi S, Yoshimoto M, et al (2000) NACP/alpha-synuclein-positive filamentous inclusions in astrocytes and oligodendrocytes of Parkinson's disease brains. Acta Neuropathol 99:14–20.

Wang Y, Zhang QJ, Liu J, et al (2010) Changes in firing rate and pattern of GABAergic neurons in subregions of the substantia nigra pars reticulata in rat models of Parkinson's disease. Brain Res 1324:54–63.

Winner B, Jappelli R, Maji SK, et al (2011) In vivo demonstration that alpha-synuclein oligomers are toxic. Proc Natl Acad Sci U S A 108:4194–4199.

Wood SJ (1999) alpha-synuclein fibrillogenesis is nucleation-dependent. J Biol harChem 274:19509–19512.